ce/papers Proceedings in civil engineering

Ernst & Sohn A Wiley Brand

ORIGINAL ARTICLE

ibausil
F. A. Finger-Institut für Baustoffkunde
Bauhaus-Universität Weimar

Effect of the pH on the interaction of hydrotalcite with dyes from textile wastewater

Martin Behringer[1] | Harald Hilbig[1] | Brigitte Helmreich[2] | Alisa Machner[1]

Correspondence

Martin Behringer, M.Sc.
Technical University of Munich
TUM School of
Engineering and Design
Department for
Materials Engineering
cbm Centre for Building Materials
Professorship for Mineral
Construction Materials
Franz-Langinger-Str. 10
81245 Munich
Email: martin.behringer@tum.de

[1] Technical University of Munich, Professorship for Mineral Construction Materials, Munich, Germany
[2] Technical University of Munich, Chair of Urban Water Systems Engineering, Garching, Germany

Abstract

The increase in textile fibre production volume is expected to result in a corresponding rise in untreated wastewater, highlighting the need for effective and affordable wastewater treatment methods. This study explored the potential of hydrotalcite, a product in cement hydration, which can be used as a low-cost adsorbent, in treating wastewater containing Reactive Blue 19 or Acid Green 1 dyes. The effect of pH on the decolourization properties was studied using HCl, HNO_3, H_2SO_4, NaOH, KOH, $Ca(OH)_2$, and $Ba(OH)_2$. The results showed that both dyes had significantly different decolourization properties with hydrotalcite in acidic and basic dye solutions, with acidic environments enhancing dye uptake. The ions present in the dye solution have no significant impact on the decolourization properties. Zeta potential analysis supported these findings, with acidic dye solutions exhibiting higher zeta potential. An intercalation of dye molecules into the layered structure of the hydrotalcite could not be detected. The study shows that hydrotalcite is most effective as an adsorbent in acidic environments.

Keywords

Textile Wastewater, Hydrotalcite, pH, Reactive Blue 19, Acid Green 1, Zeta Potential, UV/VIS

1 Introduction

The global production volume of textile fibres has more than quadrupled in the last 50 years [1]. When dyeing these textile fibres, up to 15 wt.% of the dyes are released as effluent in the process [2]. Consequently, when not treated properly, dyes pollute water sources and are a hazard to living organisms [3]. Fabric production consists of numerous different steps next to the actual dyeing step. Details on these sequences are not commonly disclosed to the public, as these steps are most often company secrets.

As modern dyes are designed to be long-lasting and resistant to light, pH changes and microbial attacks [4], thorough removal of dyes from, e.g. wastewater can be challenging. In wastewater treatment, the adsorption process is often considered convenient and simple due to its capability of removing dissolved pollutants [5; 6]. The used adsorbents range from charcoal [7] over activated carbon [8] to peat [9] and various plant products [10; 11]. Although activated carbon has been widely used as an adsorbent for several years, as it can adsorb a variety of dyes [12], it comes at a relatively high cost [13]. Cementitious materials, however, also offer high adsorption activity, are cheap and easy to produce, and their function as a filter is independent of their shape. Dye removal from wastewater by hydrotalcite, a hydration phase of slag-containing cement, has been studied by various authors [14–20]. With its possibility to exchange interlayer anions [21] and good adsorption properties [18], it is a promising candidate for dye removal from textile wastewater.

While many studies have investigated the adsorption kinetics and maximum dye uptake of hydrotalcite [14; 18; 22], our study focuses less on absolute values of dye uptake but more on a comparison of uptake mechanisms in different environments regarding the pH level. A previous study has determined the optimum pH value to be around 2 [20], which is not relevant to textile wastewater treatment, where pH values from 4 up to 14 are reported [23].

While it is generally accepted that dyes do most often not intercalate into the interlayer of hydrotalcite and primarily undergo physical adsorption [17], previous papers have not explored differences in adsorption behaviour between different dye classes [15; 16; 18]. The present study also includes investigations of the effect of different bases and acids on pH and ion concentration and, thereby, on the adsorption process. Finally, we used zeta potential measurements to evaluate the role of electrostatic forces in the adsorption process, a factor that has not been examined systematically in the literature. To investigate the effect of

https://doi.org/10.1002/cepa.2936

various types of dyes, we used a reactive dye (Reactive Blue 19) and an acid dye (Acid Green 1) in this study.

2 Experimental

2.1 Materials

The hydrotalcite was synthesized according to a modified version of the method described by Reichle [24]. A solution of 0.3 mol magnesium nitrate hexahydrate and 0.15 mol aluminium nitrate nonahydrate in 210 mL deionized water (<1 µS) was added to a solution of 1.05 mol, 50 % sodium hydroxide (aq.) and 0.283 mol sodium carbonate in 300 mL deionized water. The addition was carried out in a 1-liter flask immersed in an oil bath equipped with a mechanical agitator, a peristaltic pump, and a thermometer. The addition took 4 h at a rate of 1.11 mL per min at a temperature of 35 °C (± 0.5 °C). The resulting slurry was then stirred at 75 ± 5 °C for 18 h. After the heating period, the slurry was cooled to room temperature, centrifuged, and the separated solid was washed three times with deionized water until the residual sodium ion content was below 1 g/L. The resulting product was then dried at 125 °C in a vacuum oven (100 mbar) for 24 h yielding 20 – 25 g of powder. Two batches of hydrotalcite were synthesized. The material was first ground in a vibratory disc mill for 20 s and afterwards in a mortar mill for three cycles of 3 min each. The resulting powder was sieved to a maximum grain size of 63 µm, with a resulting d_{50} value of 11 µm and a standard deviation of 2 µm. The synthesized hydrotalcite was characterized by X-Ray diffraction (XRD) to confirm its composition and purity. The particle size distribution of the synthesized hydrotalcite was determined using a Mastersizer 3000 by Malvern.

Remazol Brilliant Blue R (Sigma Aldrich; chemical formula: $C_{22}H_{16}N_2Na_2O_{11}S_3$, molar mass of 626.54 g/mol, water solubility is 1 mg/mL), also known as Reactive Blue 19 (RB19), was used as a reactive dye and belongs to the anthraquinone dye class. Naphthol Green B (Alfa Aesar; chemical formula: $C_{30}H_{15}FeN_3Na_3O_{15}S_3$, molar mass: 878.47 g/mol, water solubility at 20 °C: 160 mg/mL), also known as Acid Green 1 (AG1), was used as an acid dye.

2.2 Methods

2.2.1 Decolourization experiments with UV-VIS spectroscopy

To conduct the decolourization experiments, 50.00 mg (± 0.05 mg) of the dye was mixed with 500 mL of deionized water. This dye concentration was chosen to ensure that the solution was not completely decolourized during the adsorption tests, but still, a sufficient change in the dye concentration of the solution was able to be analysed with UV/VIS. Different bases and acids were added to adjust the initial pH of the solution to 5 (± 0.3) and 11 (± 0.1) using a Schott ProLab 400 with a SI Analytics pH-combination electrode N65. The targeted pH values were chosen based on common pH values reported in textile wastewaters [23]. The bases used were 1.0 mol/L KOH, 1.0 mol/L NaOH, saturated (1.7 g/l) $Ca(OH)_2$, and 1.0 mol/L $Ba(OH)_2$, while the acids used were 0.1 mol/L HCl, 0.1 mol/L HNO_3, and 0.1 mol/L H_2SO_4. Two sets of decolourization experiments were conducted, one where the pH was set only initially and the hydrotalcite was subsequently added, and another where the pH was maintained constant throughout the experiment. 200 mg of hydrotalcite was added to the 500 ml dye solutions for each decolourization experiment.

A Perkin-Elmer Lambda 465 UV-VIS spectrometer with an 8-channel flow-through cell, coupled with an ALS PCP 151L Metering Pump, was used to measure the decolourization of the solution in situ as a function of time. To prevent solid material from entering the hoses, and so the analysis chamber, we used 10 µm UHMW polyethylene cannula filters (Erweka), which were tested beforehand to ensure that they did not adsorb any dye. The experiment was carried out for a duration of 3 h, and calibration curves were measured beforehand to calculate the dye concentration from the measured absorption. The initial measurement frequency was every minute for the first 10 minutes, followed by measurements every 5 minutes for the first hour, and then every ten minutes for the remaining two hours. The measurements were performed on a single cell at a time, utilizing an automated sample changer. The entire spectrum was recorded at each measurement time, but for illustration of the data, a specific wavelength (585 nm for RB19 and 600 nm for AG1) with a low noise level was chosen. The initial dye concentration was known for every measurement. To adjust for slight variations in the measured intensity, the first measurement value was always set to 100 % after measuring a blank and baseline. For the evaluation of the raw data, we used IDISis software (Automated Lab Systems).

After each decolourization experiment, the suspension containing the dye-stained hydrotalcite was filtered using a type 598 round filter. The resulting solid phase was stored in a snap-top glass vial at room temperature for further analysis.

2.2.2 Zeta potential

A Dispersion Technology 1200 measurement device was used to measure the zeta potential using the electroacoustic method, alongside the pH using a Metrohm LL-Solitrode. The temperature remained constant at 20 °C throughout the measurements. Measurements were conducted in a 150 mL glass beaker with magnetic stirring. 5 mg of dye was diluted in 50 mL of deionised water. HCl, KOH, and $Ca(OH)_2$ were titrated to maintain a constant pH value. We opted to increase the weight fraction of hydrotalcite to 1 wt.% because it represents the threshold between the suitability for the electrophoretic and electroacoustic methods [25]. This enables comparison tests between the two test methods in the future.

The zeta potential was calculated with the determination of the electrophoretic mobility (CVI). After setting the initial pH, hydrotalcite was added to the dye solution, and up to 15 measurements were taken within 20 min. To ensure reproducible results, the hydrotalcite concentration was increased to 1 wt.% (10 g/L) compared to the 0.04 wt.% (0.4 g/L) in the UV/VIS experiments. The zeta potential value at 10 min was chosen as the decisive value.

2.3 X-ray diffraction

XRD analysis was used to determine whether the dye was adsorbed onto the surface of the hydrotalcite or intercalated into the layered structure. By measuring the change in interlayer distance, XRD provided insight into the location of the dye within the hydrotalcite structure. A Bruker D8 Advance X-ray diffractometer (Cu-tube with 1.5418 Å wavelength and a LYNXEYE_XE_T detector) was used to characterize the hydrotalcite before and after dye adsorption. The XRD measurements were performed over a 2-Theta range of 5-70 °, a step size of 0.02 ° and a measurement time of 0.2 s/step. Measurements were carried out on a Si low background sample holder due to the small sample size.

3 Results and discussion

With the measured absorption and its above-mentioned calibration, we calculated the decolourization [mg adsorbed dye per g hydrotalcite].

In the first decolourization experiments, we used four bases (NaOH, KOH, $Ca(OH)_2$, $Ba(OH)_2$) and three acids (HCl, HNO_3, H_2SO_4) to determine their potential effect on the decolourization efficacy of hydrotalcite. No pH adjustments were made after hydrotalcite was added and during the decolourization process.

The UV/VIS results showed significant differences between the bases and acids in terms of their decolourization efficiencies for both dyes (cf. Figure 1 & Figure 2). The decolourization process exhibited an initial rapid phase, followed by a slower phase leading to a plateau after approximately one h. At this stage, the excess dye in the solution suggested that the maximum adsorption capacity had been reached for the given concentration. Interestingly, samples containing $Ca(OH)_2$ and $Ba(OH)_2$ appeared to adsorb more dye than samples containing the other bases. This was at first counterintuitive, as we expected the decolourization to be mainly controlled by the OH^- or H^+ present in the solution and not the counterparts of the bases or acids. However, XRD analysis of the dyed solid showed the presence of $BaCO_3$ and $CaCO_3$, which could have interfered with the measurements. To confirm this, we analysed the UV/VIS spectra of the dye-stained water (green and blue) and added $Ba(OH)_2$ to the solution. The addition of $Ba(OH)_2$ slightly changed the UV/VIS spectra, indicating that the presence of $BaCO_3$ and $CaCO_3$ had indeed affected the measurements.

Furthermore, the graphs of AG1 and RB19 show a difference in their total dye uptake. RB19 is more effectively adsorbed than AG1, possibly due to the different functional groups present in the molecules. While both dyes have hydroxyl and sulfonate groups, AG1 has three nitroso groups, while RB19 has two amino groups, which may affect the adsorption behaviour. Different functional groups of dyes may affect properties like dye-fibre fixation, substantivity or stability towards acid hydrolysis [26]. In addition, the different molecular sizes and shapes of the dyes may play a role. Planar molecules, such as RB19, are likely more easily adsorbed, as π-π-stacking of aromatic rings has been observed to positively influence dye adsorption as van der Waals, dipole and hydrogen bonds are maximised [27; 28]. Finally, differences in the surface charge of hydrotalcite could also contribute to the varying adsorption behaviour. The solubility in water was high for both dyes, and the pH of the solution was controlled in the same manner, suggesting that these factors did not play a role in the observed differences between the two dyes.

We observed a slight increase in decolourization efficiency for the acids after 20 min, prompting further investigation. To this end, we repeated the experiment and extracted 20 mL of the liquid phase before and after the observed increase at 20 and 90 min, which were subsequently analysed via ICP-OES. The analysis revealed a slight increase in Mg and Al in the dye solution at 90 min compared to the solution at 20 min. One possible explanation for this observation is that more hydrotalcite was ground by the magnetic stirrers, resulting in increased dilution of Mg and Al. However, if this were the case, we would expect to see this effect for all curves and not only at a pH value of 5. Therefore, the slight increase in decolourization after 20 min remains unclear to the authors.

Despite testing several different acids, no significant differences were observed between their decolourization efficiency. Similarly, only minor variations were observed in the monovalent bases, while the divalent bases exhibited differences that were more pronounced. Upon adding hydrotalcite to the solution, the pH value quickly shifted towards the equilibrium pH of hydrotalcite in the solution, 9.5. Any adjustments made to the initial pH had little impact on the final pH values, which averaged 10.5 (± 0.3)

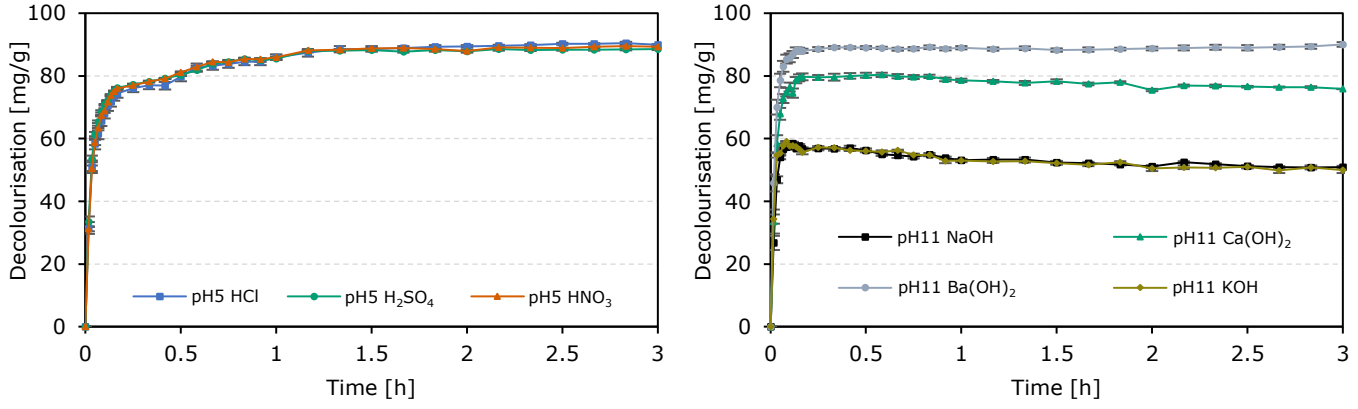

Figure 1 Dye adsorption in mg dye per g of hydrotalcite for Reactive Blue 1 for the acids (left) and bases (right) measured at 585 nm. The error bars indicate the standard error (n=3)

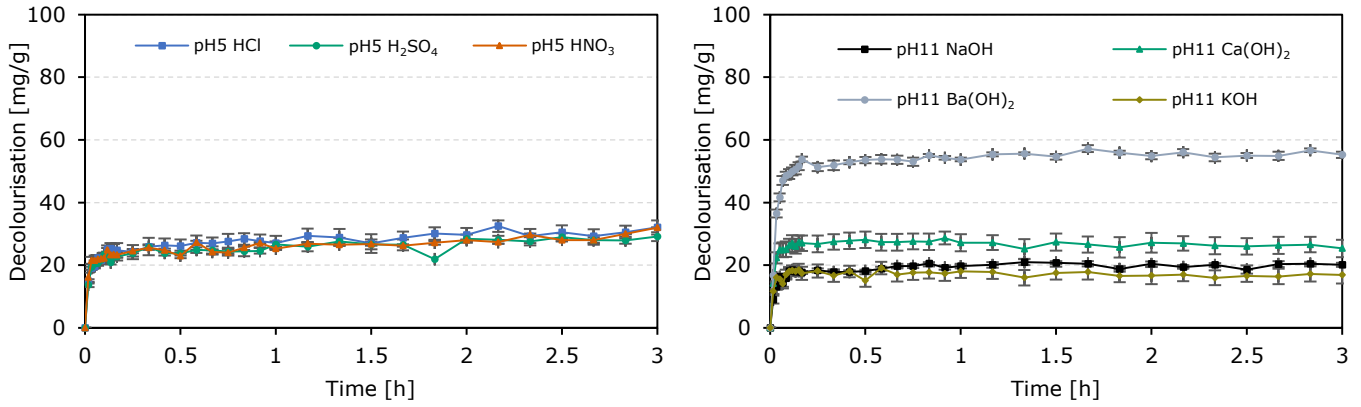

Figure 2 Dye adsorption in mg dye per g of hydrotalcite for Acid Green 1 for the acids (left) and bases (right) measured at 600 nm. The error bars indicate the standard error (n=3)

for all batches with bases and 8.9 (± 0.5) for all batches with acids. To further investigate the effects of pH, we conducted additional experiments with HCl, KOH, and $Ca(OH)_2$, in which we maintained a constant pH after the addition of hydrotalcite (cf. Figure 3).

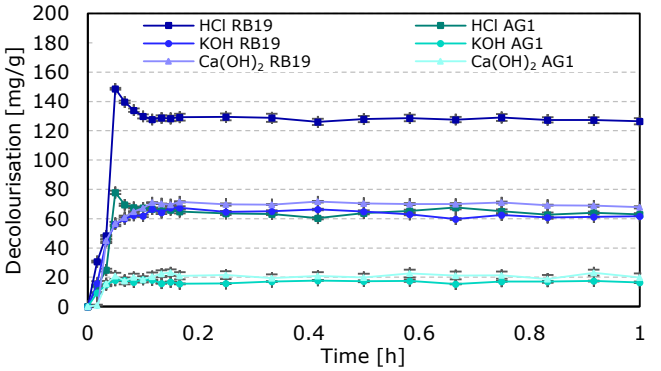

Figure 3 Dye adsorption in mg dye per g of hydrotalcite for Reactive Blue 19 and Acid Green 1 at a constant pH value. The error bars indicate the standard error (n=3)

The results from the decolourization experiment (cf. Figure 3) showed that the acidic batches – now as the pH is kept constant – had a higher potential for decolourization compared to the previous experiment. Figure 3 indicated that HCl had almost 50% higher decolourization potential for RB19 and 90% higher potential for AG1 compared to the setup where only the initial pH value was set. The decolourization potential of $Ca(OH)_2$ and KOH did not exhibit significant differences across the dyes. This difference between decolourization efficiency in Figure 1 and Figure 2 compared to Figure 3 could be attributed to the availability of metal ions in the solution. At higher pH values, the solubility of carbonates decreases [29], resulting in more Ca^{2+}/Ba^{2+} ions present in the liquid phase at low pH values. We hypothesize that these metal ions form coordination complexes with dye molecules. In this scenario, the metal ion (e.g. Ca^{2+} or Ba^{2+}) acts as the central ion, which is surrounded by a group of ligands (e.g. sulfonate groups of AG1 or RB19). However, further studies are required to validate this hypothesis and examine the specific mechanisms through which metal-dye complexes are formed and contribute to the decolourization process.

However, we did observe some additional peaks for the sample containing $Ba(OH)_2$ (cf. Figure 4 at ~24° 2θ) and $Ca(OH)_2$, which we attributed to the formation of their respective carbonates, $BaCO_3$ and $CaCO_3$, during the decolourization experiment.

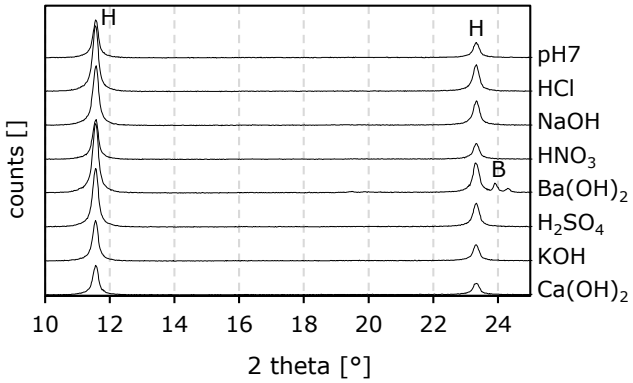

Figure 4 – XRD diffractograms in the range of 10-25° 2θ of hydrotalcite after decolourization experiments in various solutions. H = hydrotalcite; B = barium carbonate

Therefore, to further investigate the mechanisms responsible for the observed differences in decolourization, we examined two main mechanisms of ion uptake of hydrotalcite that have been reported in the literature: physical adsorption (cf. Introduction) and intercalation [30; 31]. Intercalation occurs when ions are incorporated into the interlayer region of hydrotalcite, leading to changes in its lattice parameters that can be observed through X-ray diffraction. To examine whether intercalation occurred, we compared the synthesized hydrotalcite with filtered hydrotalcite after the decolourization experiments. Our analysis indicated no changes in lattice parameters for the analysed samples (cf. Figure 4), suggesting that no intercalation took place. Consequently, the decolourization shown by the UV/VIS results has to be due to the adsorption of dyes on the hydrotalcite surface.

We, therefore, excluded the effects of intercalation and focused on understanding the factors that contribute to physical adsorption. To investigate the observed differences in physical adsorption, we conducted zeta potential measurements during the decolourization experiments. Although these quantities are not absolute values, they can be compared relative to each other. It is important to note that zeta potential is highly dependent on the available surface area, thus on the particle size distribution and the weight percentage of solids in the solution.

When a charged particle is dispersed in water, a layer model is used to explain the adsorption process based on Helmholtz and Stern [32; 33]. In Figure 5 and Figure 6, the different layers are presented for the case of a high

and a low zeta potential. When diffusion movements occur in a solution, a part of the diffuse layer is stripped off due to friction, and the measured potential is, therefore, no longer neutral in charge, which is the zeta potential.

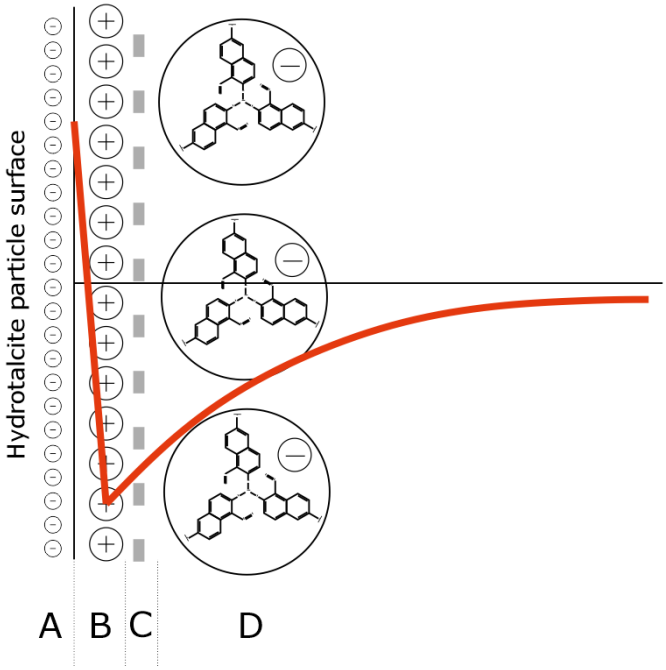

Figure 5 Potential curves of the surface of a negatively charged hydrotalcite particle for a high zeta potential. (A) displays the negatively charged particle surface; (B) is the Stern layer containing dehydrated ions; (C) represents the shear plane; (D) displays the diffuse layer, which accommodates the negatively charged dye molecules (Acid Green 1).

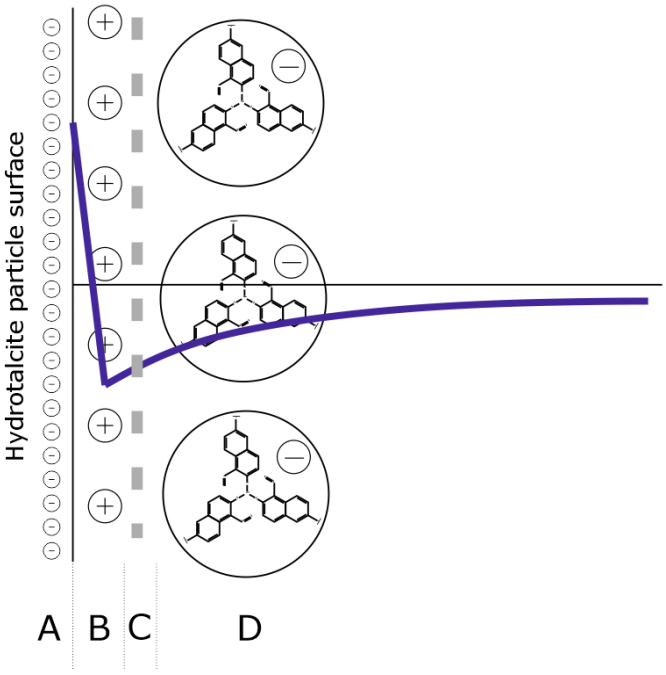

Figure 6 Potential curves of the surface of a negatively charged hydrotalcite particle for a low zeta potential. (A) displays the negatively charged particle surface; (B) is the Stern layer containing dehydrated ions; (C) represents the shear plane; (D) displays the diffuse layer, which accommodates the negatively charged dye molecules (Acid Green 1)

In Figure 7, it can be observed that the zeta potential of acidic solutions (~50 mV) is higher than that of alkaline solutions for both studied dyes. This can be explained by the accumulation of the positive charge of H^+ ions in the Stern layer due to the negatively charged hydrotalcite particle surface. The positive zeta potential measurement suggests a positive Stern potential (ψi), while the negatively charged dyes accumulate in the diffuse layer. Compared to HCl, samples prepared with $Ca(OH)_2$, $Ba(OH)_2$, or KOH show significantly lower zeta potentials. This is due to the lack of small positively charged ions (H^+) in the solution in the basic environment, resulting in a lower ψi, as the inner Helmholtz layer is less densely populated. Moreover, the ion radius of H^+ is considerably smaller than Na^+ or K^+ ions, leading to a smaller potential drop, illustrated in Figure 6. The UV/VIS results support these findings, as they demonstrate that acidic solutions are more effective than alkaline solutions in terms of dye uptake.

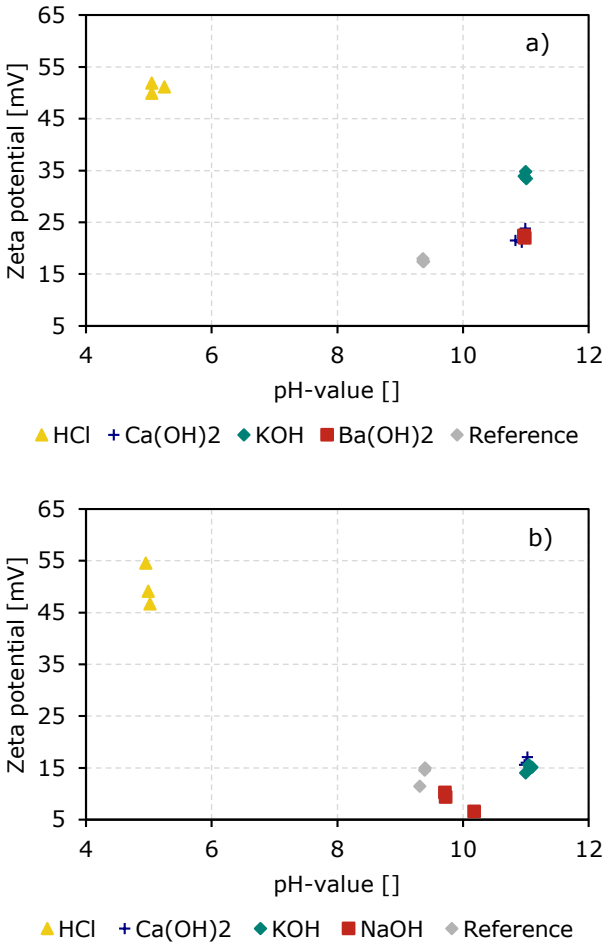

Figure 7 Zeta potential of 0.5 g Hydrotalcite diluted in 50 ml dye solution for RB19 (a) and AG1 (b) for different bases, acids, and a reference without pH adjustments

However, it is not conclusive that this is due to a negatively charged hydrotalcite particle. Another possible explanation is that the particle surface of hydrotalcite may be positive in an acidic environment. This would make it unlikely for hydrogen ions to accumulate onto the particle surface as positively charged ions have a higher hydration number than ions with a negative charge. This is because it is harder for the ion to strip off the hydrate shell in case of a higher hydration number.

As a result, the van der Waals forces between the particle surface and the ions on the inner Helmholtz plane are not

as strong, allowing negatively charged dye ions to accumulate onto the Stern layer. However, the authors were not able to provide conclusive evidence to support either theory, highlighting the need for further research. Nonetheless, it is important to note that in both scenarios, the shear plane of hydrotalcite has a net positive charge in all cases tested, hence a positive zeta potential. Furthermore, the potential in the Stern layer is increasing with decreasing pH values, which is consistent with the observed increase in decolourization potential.

While the zeta potential measurements helped to explain the differences in dye uptake in the presence of acids and bases, it remains inconclusive as to why the uptake of AG1 is significantly lower than that of RB19. While both dyes have similar zeta potential values, the authors suggest that the difference in uptake is more likely due to the size and shape of the dye molecules and their respective functional groups. One possible approach to verify this assumption is to carry out decolourization experiments using organic compounds with a single functional group and still exhibit a detectable UV/VIS spectrum.

4 Conclusion

This study investigated the relationship between the pH and the decolourization potential of hydrotalcite in solution with the two dyes, Reactive Blue 19 and Acid Green 1. Four bases (NaOH, KOH, $Ca(OH)_2$, and $Ba(OH)_2$) and three acids (HCl, HNO_3, and H_2SO_4) were used to determine their effect on the decolourization efficiency of hydrotalcite.

The results showed that both dyes had significantly different decolourization properties in acidic and basic dye solutions with hydrotalcite, with acidic environments enhancing the dye uptake. The ions present in the dye solution did not appear to have a big impact on the decolourization properties, except for $Ba(OH)_2$ and $Ca(OH)_2$, where divalent bases showed higher decolourization efficiencies than the monovalent bases. For the divalent bases, however, carbonates formed during the experiment, which appeared to have affected the results. Minimizing the CO_2 uptake in a dye solution with a high pH value of 11 reduces the production of carbonates and results in a smaller difference between monovalent and divalent bases.

The higher zeta potential observed in acidic, compared to basic, dye solutions supports the previous findings. It indicates that the presence of H^+ and OH^- in the solution is the main factor controlling the differences in dye uptake, where H^+ ions seem to have a positive effect on the decolourization properties.

5 Acknowledgement

We would like to thank the German Research Foundation (DFG) for funding the joint project HI 1256/6-1 and HE 2413/9-1. The authors would like to thank Tanja Ertl, Roya Rafiee Tary and Hady Elhashmy for their help with sample preparation and conducting the experiments.

References

[1] Industrievereinigung Chemiefaser Production volume of chemical and textile fibers worldwide from 1975 to 2021 (in 1,000 metric tons) [Graph] in: Die Chemiefaserindustrie in der Bundesrepublik Deutschland: 2021/2022.

[2] Galindo, C.; Jacques, P.; Kalt, A. (2001) *Photooxidation of the phenylazonaphthol AO20 on TIO2: kinetic and mechanistic investigations* in: Chemosphere 45, 6-7, pp. 997–1005. https://doi.org/10.1016/S0045-6535(01)00118-7

[3] Kant, R. (2012) *Textile dyeing industry an environmental hazard* in: Natural Science 04, Nr. 01, pp. 22–26. https://doi.org/10.4236/ns.2012.41004

[4] PAGGA, U. (1994) *Development of a method for adsorption of dyestuffs on activated sludge* in: Water research 28, H. 5, pp. 1051–1057. https://doi.org/ 10.1016/0043-1354(94)90190-2

[5] Gisi, S. de et al. (2016) *Characteristics and adsorption capacities of low-cost sorbents for wastewater treatment: A review* in: Sustainable Materials and Technologies 9, pp. 10–40. https://doi.org/10.1016/ j.susmat.2016.06.002

[6] Wang, J.; Guo, X. (2020) *Adsorption isotherm models: Classification, physical meaning, application and solving method* in: Chemosphere 258. https://doi.org/10.1016/j.chemsphere.2020.127279

[7] Bangash, F. K.; Manaf, A. (2005) *Dyes Removal from Aqueous Solution Using Wood Activated Charcoal of Bombax Cieba Tree* in: Journal of the Chinese Chemical Society 52, H. 3, pp. 489–494. https://doi.org/10.1002/jccs.200500070

[8] Rodríguez, A. et al. (2009) *Adsorption of anionic and cationic dyes on activated carbon from aqueous solutions: equilibrium and kinetics* in: Journal of hazardous materials 172, 2-3, pp. 1311–1320. https://doi.org/10.1016/j.jhazmat.2009.07.138

[9] Allen, S. J.; McKay, G.; Porter, J. F. (2004) *Adsorption isotherm models for basic dye adsorption by peat in single and binary component systems* in: Journal of colloid and interface science 280, Nr. 2, pp. 322–333. https://doi.org/10.1016/j.jcis.2004.08.078

[10] Doulati Ardejani, F. et al. (2007) Numerical modelling and laboratory studies on the removal of Direct Red 23 and Direct Red 80 dyes from textile effluents using orange peel, a low-cost adsorbent in: Dyes and Pigments 73, H. 2, pp. 178–185. https://doi.org/10.1016/j.dyepig.2005.11.011

[11] Bhattacharyya, K. (2003) *Adsorption characteristics of the dye, Brilliant Green, on Neem leaf powder* in: Dyes and Pigments 57, H. 3, pp. 211–222. https://doi.org/10.1016/S0143-7208(03)00009-3

[12] Babel, S. (2003) *Low-cost adsorbents for heavy metals uptake from contaminated water: a review* in: Journal of hazardous materials 97, 1-3, pp. 219–243. https://doi.org/10.1016/S0304-3894(02)00263-7

[13] Yagub, M. T. et al. (2014) *Dye and its removal from*

aqueous solution by adsorption: a review in: Advances in colloid and interface science 209, pp. 172–184. https://doi.org/10.1016/j.cis.2014.04.002

[14] Heraldy, E. et al. (2015) *Anionic and Cationic Dyes Removal from Aqueous Solutions by Adsorption onto Synthetic Mg/Al Hydrotalcite-Like Compound* in: Indonesian Journal of Chemistry 15, H. 3, pp. 234–241. https://doi.org/10.22146/ijc.21190

[15] Orthman, J.; Zhu, H.; Lu, G. (2003) *Use of anion clay hydrotalcite to remove coloured organics from aqueous solutions* in: Separation and Purification Technology 31, H. 1, pp. 53–59. https://doi.org/10.1016/S1383-5866(02)00158-2

[16] Sriram, G. et al. (2020) Mg–Al-Layered Double Hydroxide (LDH) Modified Diatoms for Highly Efficient Removal of Congo Red from Aqueous Solution in: Applied Sciences 10, H. 7. https://doi.org/10.3390/app10072285

[17] Bascialla, G.; Regazzoni, A. E. (2008) *Immobilization of anionic dyes by intercalation into hydrotalcite* in: Colloids and Surfaces A: Physicochemical and Engineering Aspects 328, 1-3, pp. 34–39. https://doi.org/10.1016/j.colsurfa.2008.06.028

[18] Malik, A. et al. (2022) Highly efficient hydrotalcite-based adsorbent for aqueous-phase cationic dye removal: structural features, kinetics and isotherm study in: International Journal of Environmental Science and Technology 20, H. 1, pp. 565–578. https://doi.org/10.1007/s13762-021-03843-9

[19] Wagner, M. et al. (2020) *Removal of Congo Red From Aqueous Solutions at Hardened Cement Paste Surfaces* in: Frontiers in Materials 7. https://doi.org/ 10.3389/fmats.2020.567130

[20] Vanaamudan, A.; Chavada, B.; P., P. (2016) *Adsorption of reactive blue 21 and reactive red 141 from aqueous solutions onto hydrotalcite* in: Journal of Environmental Chemical Engineering 4, H. 3, pp. 2617–2627. https://doi.org/10.1016/j.jece.2016.04.039

[21] Evans, D. G.; Slade, R. C. T. (2006) *Structural Aspects of Layered Double Hydroxides* in: Duan, X.; Evans, D. G. [Eds.] *Layered double hydroxides*. Berlin, Heidelberg: Springer, pp. 1–87.

[22] Lazaridis, N. K.; Karapantsios, T. D.; Georgantas, D. (2003) *Kinetic analysis for the removal of a reactive dye from aqueous solution onto hydrotalcite by adsorption* in: Water research 37, H. 12, pp. 3023–3033. https://doi.org/10.1016/S0043-1354(03)00121-0

[23] Dey, S.; Islam, A. *A Review on Textile Wastewater Characterization in Bangladesh* in: Resources and Environment 2015, 5(1), pp. 15–44. https://doi.org/10.5923/j.re.20150501.03

[24] REICHLE, W. (1985) *Catalytic reactions by thermally activated, synthetic, anionic clay minerals* in: Journal of Catalysis 94, H. 2, pp. 547–557. https://doi.org/10.1016/0021-9517(85)90219-2

[25] Dukhin, A. S.; Xu, R. (2020) *Zeta-potential measurements* in: Hodoroaba, V.-D.; Unger, W. E. S.; Shard, A. G. [Eds.] *Characterization of nanoparticles: Measurement processes for nanoparticles*. Amsterdam, Oxford, Cambridge, MA: Elsevier, pp. 213–224.

[26] Clark, M. (2011) Fundamental principles of dyeing in: Clark, M. [Ed.] Handbook of Textile and Industrial Dyeing: Principles, Processes And Types Of Dyes. Burlington: Elsevier Science, pp. 3–27.

[27] Zhao, C. et al. (2021) A novel surface-active monomer decorating a self-floating adsorbent with high pH adaptability for anionic dyes: π-π stacking in: Journal of Molecular Liquids 321. https://doi.org/10.1016/ j.molliq.2020.114864

[28] Chattopadhyay, D. P. (2011) Chemistry of dyeing in: Clark, M. [Ed.] Handbook of Textile and Industrial Dyeing: Principles, Processes And Types Of Dyes. Burlington: Elsevier Science, pp. 150–183.

[29] Hart, P. W.; Colson, G.; Burry, J. (2012) *Application of Carbon Dioxide to reduce water side lime scale in heat exchanges* in: Pulp and Paper Canada -Ontario- 1(2), pp. 67–70.

[30] Tamura, H. et al. (2006) *Formation of hydrotalcite in aqueous solutions and intercalation of ATP by anion exchange* in: Journal of colloid and interface science 300, Nr. 2, pp. 648–654. https://doi.org/10.1016/j.jcis.2006.04.007

[31] Yang, C. et al. (2016) *Synthesis and characterization of Mn intercalated Mg-Al hydrotalcite* in: Journal of colloid and interface science 479, pp. 115–120. https://doi.org/10.1016/j.jcis.2016.06.057

[32] Helmholtz, H. (1853) Ueber einige Gesetze der Vertheilung elektrischer Ströme in körperlichen Leitern mit Anwendung auf die thierisch-elektrischen Versuche in: Annalen der Physik und Chemie 165, H. 6, pp. 211–233. https://doi.org/10.1002/andp.18531650 603

[33] Stern, O. (1924) *ZUR THEORIE DER ELEKTROLYTISCHEN DOPPELSCHICHT* in: Zeitschrift für Elektrochemie und angewandte physikalische Chemie 30, 21-22, pp. 508–516.